Molecular Ecology (2006) **15**, 4513–4531 doi: 10.1111/j.1365-294X.2006.03107.x

A tale of two flatties: different responses of two terrestrial flatworms to past environmental climatic fluctuations at Tallaganda in montane southeastern Australia

PAUL SUNNUCKS,*§ MARK J. BLACKET,*¶ JODY M. TAYLOR,*§ CHESTER J. SANDS,* SHERRYN A. CIAVAGLIA,* RYAN C. GARRICK,* NOEL N. TAIT,† DAVID M. ROWELL‡ and ALEXANDRA PAVLOVA§

*Department of Genetics, La Trobe University, Bundoora, Vic. 3086, †Department of Biological Sciences, Macquarie University, Sydney, NSW 2109, ‡School of Botany and Zoology, Australian National University, Canberra, ACT 0200, Australia §School of Biological Sciences and Australian Centre for Biodiversity: Analysis, Policy and Management, Monash University, Clayton, Vic. 3800, Australia

Abstract

Comparative phylogeographic studies of animals with low mobility and/or high habitat specificity remain rare, yet such organisms may hold fine-grained palaeoecological signal. Comparisons of multiple, codistributed species can elucidate major historical events. As part of a multitaxon programme, mitochondrial cytochrome oxidase I (COI) variation was analysed in two species of terrestrial flatworm, *Artioposthia lucasi* and *Caenoplana coerulea*. We applied coalescent demographic estimators and nested clade analysis to examine responses to past, landscape-scale, cooling-drying events in a model system of montane forest (Tallaganda). Correspondence of haplotype groups in both species to previously proposed microbiogeographic regions indicates at least four refuges from cool, dry conditions. The region predicted to hold the highest quality refuges (the Eastern Slopes Region), is indicated to have been a long-term refuge in both species, but so are several other regions. Coalescent analyses suggest that populations of *A. lucasi* are declining, while *C. coerulea* is expanding, although stronger population substructure in the former could yield similar patterns in the data. The differences in spatial and temporal genetic variation in the two species could be explained by differences in ecological attributes: *A. lucasi* is predicted to have lower dispersal ability but may be better able to withstand cold conditions. Thus, different contemporary population dynamics may reflect different responses to recent (Holocene) climate warming. The two species show highly congruent patterns of catchment-based local genetic endemism with one another and with previously studied slime-mould grazing Collembola.

Keywords: comparative phylogeography, flatworm, Great Dividing Range, mitochondrial DNA, saproxylic, Tallaganda

Received 4 April 2006; revision accepted 26 July 2006

Introduction

The increasing sophistication of molecular population biology has facilitated a growing appreciation of the complexity and variability of forces that generate and maintain biological diversity in different situations (Avise & Walker 1998; Trewick & Wallis 2001; Knowles & Maddison 2002). Many mobile and ecologically nonspecialist taxa show little genetic structuring, while less mobile and more specialist taxa may be extremely finely differentiated, showing a profound influence of landscape history and climate change (Hewitt 2004a, b). For example, where large areas of formerly inhospitable habitat become quickly available for colonization, low genetic structure is often detected (Ayoub & Riechert 2004; Smith & Farrell 2005), whereas specialized, nonvagile taxa in stable and complex landscapes tend to show strong structure (e.g. Cooper *et al*. 2002; Hugall *et al*. 2002).

Saproxylic (dead wood-dependent) communities offer very interesting terrestrial models in these contexts, because their relatively immobile, habitat-specific taxa (references in Garrick *et al*. 2004) may exhibit genetic signatures of

Correspondence: Paul Sunnucks, Fax: Number: 61 3 99055613; E-mail: paul.sunnucks@sci.monash.edu.au
¶Present address: CESAR/Department of Genetics, University of Melbourne, Parkville, Vic. 3010, Australia.

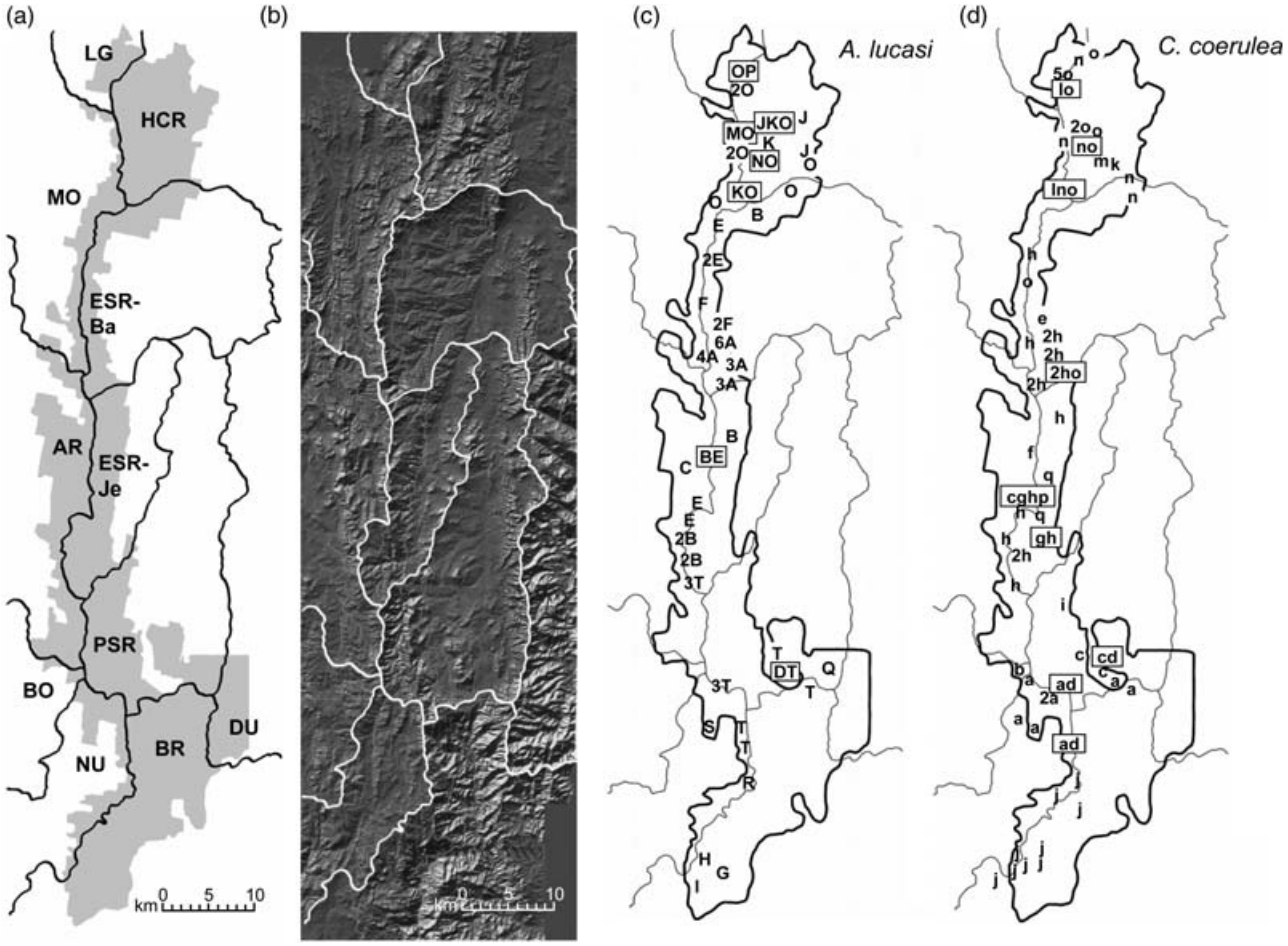

Fig. 1 (a) Sub-catchment-based microbiogeographical regions (delineated with black lines) within Tallaganda (grey shading). Lake George catchment: LG, Lake George; Shoalhaven catchment: HCR, Harolds Cross Region, ESR, Eastern Slopes Region (Ba, Ballalaba and Je, Jerrabatgulla subcatchments), PSR, Pikes Saddle Region; Deua catchment: DU, Deua; Tuross catchment: BR, Badja Region; Murrumbidgee catchment: NU, Numeralla, BO, Bredbo, AR, Anembo Region, MO, Molonglo. (b) Relief of Tallaganda, lines indicate subcatchment-based microbiogeographical regions. (c and d) Approximate geographic distribution of sampling logs and haplotypes for *Artioposthia lucasi* (c) and *Caenoplana coerulea* (d). Letters on maps correspond to haplotypes (Fig. 2), their placement on the map indicate logs where a single haplotype was sampled, numbers before letters show number of neighbouring logs with the same haplotype, boxes are drawn to indicate logs where > 1 haplotype was sampled. Relief image modified from State Forests of New South Wales (1995) Proposed forestry operations in the Queanbeyan and Badja Management Area, environmental impact statement. State Forests of New South Wales, southern region.

prior climatic and geographical events that are lost in other kinds of organisms (Pfenninger & Posada 2002). Fine-scale phylogeographic patterns will permit accurate inference of the positions of biogeographic zones (Schauble & Moritz 2001). Thus, invertebrates, particularly those with limited mobility, may be excellent indicators of patterns of biodiversity in larger more mobile organisms, but the converse may not be true (Moritz *et al*. 2001; Garrick *et al*. 2006).

For these reasons, and because terrestrial, temperate Southern Hemisphere ecosystems are barely represented in the literature (Hewitt 2004a, b), we are conducting a comparative phylogeographical research programme into saproxylic invertebrates in the Tallaganda region of New South Wales, Australia (Barclay *et al*. 2000a, b; Sunnucks *et al*. 2000a; Sunnucks & Tait 2001; Garrick *et al*. 2004; Garrick & Sunnucks 2006; Woodman *et al*. 2006; Beavis & Rowell 2006). Details of the region as a research model are given in Garrick *et al*. (2004). Briefly, Tallaganda is an ecologically and physically isolated side-branch of the Great Dividing Range approximately 100 km long and currently extensively forested. The Gourock Range, the spine of Tallaganda, has remained geologically stable for > 70 million years. On the basis of drainage catchments, Garrick *et al*. (2004) identified five 'microbiogeographic' regions (named on Fig. 1a), which are estimated to have been differently impacted by cooling and drying during the Pliocene (3–5 million years ago), and approximately 20 cycles of glaciation during the Pleistocene (< 1.8 million years ago). In cold, dry conditions the tree line may have fallen by > 1000 m, reducing most of Tallaganda to treeless

steppe. Nonetheless, deep sheltered valleys potentially provided areas of forest refuge. Protected locations should have been most numerous in Eastern Slopes Region (ESR) owing to its easterly orientation and ameliorating coastal influences (Fig. 1b). We predict that ESR should present evidence (such as high diversity, local subdivision and sequences interior in networks) of being repeatedly the most important refuge from cool, dry conditions, and that the five microbiogeographic regions would be discernible in organisms that do not readily undergo movement between drainages during moister, warmer periods. Saproxylic taxa at Tallaganda must have followed moist forests to lower elevations as they retreated during cool, dry periods. Thus, this temperate fauna of modest altitude is interesting to compare with high elevation refuge systems elsewhere (e.g. Knowles 2001; Trewick & Wallis 2001; De Chaine & Martin 2004).

In this study we examine phylogeographic patterning in two codistributed terrestrial flatworms (Platyhelminthes, Tricladida, Terricola), *Artioposthia lucasi* (Dendy 1891) and *Caenoplana coerulea* Moseley (1877), genera thought to be Gondwanan relicts (Winsor 1998a). These flatworms have few morphological characters and so have uncertainly known distributions in southeastern Australia. *A. lucasi* is considered more sedentary than *C. coerulea*, being about half its weight and with very sticky mucus, while *C. coerulea* has a ciliated creeping sole providing for rapid locomotion (L. Winsor, personal communication). Thus, we predict that *A. lucasi* should show deeper genetic divergences and greater local endemism than *C. coerulea*.

Alongside the rest of our suite of saproxylic organisms [Collembola (springtails), Onychophora (velvet worms), and Mygalomorphae (funnel-web spiders)], terrestrial flatworms represent organisms of intermediate 'mobility' (= dispersal ability plus ecological tolerance): their ability to move through soil and leaf litter (Winsor 1998b), their covering of mucus, and tanned egg-cocoons could help promote dispersal, persistence and gene flow. Nonetheless, Terricola are still prone to desiccation, sensitive to sunlight and heat, and reliant on invertebrate prey (Winsor 1998a, b; Sluys 1999). Thus, we would predict that genetic structuring of the two species, particularly *C. coerulea* (see above), would be shallower than that of two species of 'giant' Collembola (Garrick *et al*. 2004; Garrick & Sunnucks 2006), but stronger than that of funnel-web spiders (Beavis & Rowell 2006). They increase the biological breadth of our target taxa in being the only hermaphrodites.

Materials and methods

Taxon sampling

Between 1997 and 2004, 197 *Artioposthia lucasi* and 192 *Caenoplana coerulea* were collected from 69 and 72 logs, respectively, along a ~100-km north–south transect through the five Tallaganda catchments (Fig. 1) and also from neighbouring catchments of Molonglo (ML), Lake George (LG), Numeralla (NU), Bredbo (BO), and Deua (DU) (Fig. 1, Appendix I). Specimens were transported live then stored at –80 °C.

DNA isolation, amplification of mitochondrial DNA and screening of haplotypes

Genomic DNA was extracted from approximately 2 mm^3 of tissue by 'salting out' (Sunnucks & Hales 1996). Approximately 450 bp of cytochrome oxidase I (COI) were amplified with primers 'FlatwormCOI-F' (5'-GCAGTTTTTGGTTTTTTGGACATCC-3') and 'FlatwormCOI-R' (5'-GAGCAACAACATAATAAGTATCATG-3'). We designed these from the M6 and M10 conserved domains of COI (Lunt *et al*. 1996) for Terricola available on GenBank (*Artioposthia* AF17805, AF17835; *Platydemus* AF178320; *Bipalum* AF178307; *Geoplana* AF178315). Unlike commonly used primers, these ones circumvented apparent multiple nuclear pseudogenes of mitochondrial DNA (mtDNA) (e.g. Sunnucks & Hales 1996). Amplifications were performed in 10 μL containing 16 μM ammonium sulphate, 68 mM Tris-HCl (pH 8), 10 mM β-mercaptoethanol, 5% bovine serum albumin 10 mg/mL (Progen), 2 mM $MgCl_2$, 200 μM each dNTP, 0.5 μM each primer, 0.5 units of *Taq* DNA Polymerase (Promega) and ~50 ng of template DNA. The amplified region spans seven structural regions of COI, including two highly variable internal loops (I3 and I4). Amplifications involved 2 min at 94 °C (1 cycle), 20 s at 94 °C, 30 s at 50 °C, 45 s at 72 °C (35 cycles), with a final 2-min extension (72 °C).

Polymerase chain reaction (PCR) amplifications to screen for individual genetic variation using single-stranded confirmation polymorphism (SSCP) were performed as above except with the addition of 0.05 μL [α^{33}P]-dATP (10 mCi/mL) (Sunnucks *et al*. 2000b). Multiple representatives of each putative haplotype (where they existed) (GenBank accession nos for *A. lucasi* haplotypes: DQ227619–35; and *C. coerulea*: DQ227636–54) were sequenced commercially (Macrogen Inc.) on an ABI automated sequencer. Haplotypes found more than once in *C. caenoplana* were sequenced a mean of 3.3 and up to 10 times, and for *A. lucasi* a mean of 3.25 and up to 8 times, without ever finding unrecognized sequence variation.

DNA sequence analysis

All sequences were edited with reference to chromatograms and aligned using CLUSTAL_X version 1.83 (Thompson *et al*. 1997). Tajima's *D* (Tajima 1989) and Fu's F_s (Fu 1997) were calculated in DNASP version 4.10 (Rozas *et al*. 2003). These tests are unable to distinguish between selection

and demographic processes (Ballard & Whitlock 2004). We were unable to apply the McDonald & Kreitman (1991) (M-K) test, which is insensitive to demographic changes when detecting purifying selection (Eyre-Walker 2002), because we had only single outgroup sequences that are close sisters of each ingroup. To assess the nature of the sequence variation, standard sequence composition data were examined (Appendix II).

The geographic scale of contemporary spatial patterning of mtDNA haplotype frequency variation within each species at Tallaganda was assessed using spatial autocorrelation in GENALEX 5.1 (Peakall & Smouse 2001), using 999 permutations and checking for similar outcomes when using different distance bins.

MODELTEST 3.06 (Posada & Crandall 1998) with Akaike information criterion (AIC) was used to determine the best-fit model of sequence evolution. The parameters for the best model were estimated on a most parsimonious tree obtained by heuristic searching with 100 addition replicates in PAUP* version 4.0b10 (Swofford 2002), and used as starting parameters for a maximum-likelihood tree search in PAUP*. Best maximum-likelihood trees were obtained using successive approximation, under which parameters for the maximum-likelihood model were re-estimated from the best tree after each run, until the same best tree and parameter values were obtained in two successive iterations. Maximum-likelihood bootstrap analysis with 1000 replicates with the best fit model and parameters estimated from the final maximum-likelihood tree was performed to estimate node stability. Sequences of flatworms morphologically indistinguishable from *A. lucasi* and *C. coerulea* collected ~150 km away in Victoria (GenBank accession nos DQ465371 and DQ465372) were used as outgroups.

To evaluate whether the sequences were evolving in a clock-like fashion, a likelihood-ratio test compared scores from maximum-likelihood trees with and without a molecular clock. The likelihood ratio was assumed to be χ^2 distributed with degrees of freedom equal to number of taxa minus two (Nei & Kumar 2000) and was calculated as $2(\ln L_{clock} - L_{no\ clock})$.

To explore genetic characteristics and demographic history of 'genetic populations' (collections of individuals sharing the same mitochondrial DNA lineage) we used ARLEQUIN version 3.01 (Excoffier *et al*. 2005) to compute nucleotide diversity (π), haplotype diversity (h), Fu's F_s, mismatch distributions, parameters for the model of population expansion [time since expansion τ, and relative population sizes before (θ_1) and after (θ_2) expansion] and for the continent-island model of demographic expansion ($\tau = 2T\mu$, $\theta = 2N\mu$ and $M = 2Nm$, where T = number of generations before spatial expansion, μ = mutation rate, N = size of deme (assumed constant) and m = fraction of individuals from a deme exchanging with other demes). The generalized least-squares approach (Schneider & Excoffier 1999) in ARLEQUIN was used to test the empirical mismatch distributions against a model of demographic (MDE) or spatial (MSE) expansion. We used DNASP to calculate R_2 (Ramos-Onsins & Rozas 2002) for detecting population growth in the same genetic populations.

A coalescent-based method implemented in FLUCTUATE version 1.4 (Kuhner *et al*. 1998) was applied to genetic populations (with > 2 haplotypes and $N > 46$ individuals) used to estimate $\theta = 2N_e\mu$ (measure of effective population size and per-site neutral mutation rate) jointly with g (population growth parameter), and to estimate θ with no growth. Search settings were: 10 short chains (10 000 steps), then five long chains (100 000 steps) sampling every 20th step, a random starting tree, transition/transversion ratio of 2.0, empirical base frequencies, and the initial value of θ set using Watterson (1975) estimate. This was repeated five times, and the mean and standard deviation calculated. Mean g minus 3 SD > 0 was considered significant evidence of growth, whereas mean g +3SD < 0 was taken as significant population decline (Lessa *et al*. 2003).

To explore genetic subdivision and contemporary levels of gene flow between catchment-based microregions, analysis of molecular variance (Excoffier *et al*. 1992) was performed on catchment-based groups of sequences; pairwise φ_{ST} values were calculated in ARLEQUIN using simple distances. Many collecting points were effectively accessible only by fire trails along watersheds, so many logs were located on microregion borders. We analysed border samples separately. One group (MO + HCR) included individuals collected within MO, HCR and on the MO-HCR border (the rationale being few samples from MO and the border). Population subdivision and gene flow were assessed for the following groups: (i) HCR-LG border, (ii) MO+HCR, (iii) MO-ESR border, (iv) ESR-Ba, (v) ESR-Je, (vi) ESR-AR border (including AR for *A. lucasi*), (vii) PSR, (viii) PSR-DU border, (ix) PSR-NU border, (x) NU, (xi) NU-BR border, (xii) BR, and (xiii) NU-BO border (Fig. 1, Appendix III).

Finally, we used nested clade analysis (NCA, Templeton 1998) to elucidate processes driving spatio-temporal genetic patterns, independent of molecular clocks. Haplotype networks for each species were constructed using statistical parsimony (Templeton *et al*. 1992) in TCS version 1.13 (Clement *et al*. 2000). Loops were resolved via maximum-likelihood trees. The nesting design was constructed by hand for use in GEODIS 2.1 (Posada *et al*. 2000). A distance matrix of geographical distances between rotting logs was calculated from geographic positioning system (GPS) coordinates in Microsoft Excel and incorporated into GEODIS files to estimate D_c and D_n. The statistical significance of these distance measures and contrast between tip (derived) and interior (older) clades within a nested clade was obtained from GEODIS by 1000 random permutations. Where distance measures were significant, the most recent inference key (11 November 2005) was used to make biological interpretations.

Results

Evidence for typical mtDNA sequence variation

The DNA alignment was 364 bp in *Artioposthia lucasi* and 361 bp in *Caenoplana coerulea*. Sequence characteristics were consistent with typical COI variation (Appendix II). We consider the sequences functional mtDNA rather than nonfunctional alternatives because (i) almost all DNA substitutions involved silent third codon position changes, (ii) sequences contained no inferred stop codons, (iii) the inferred amino acid sequences fit the Lunt *et al*. (1996) structural model, (iv) the indel between the two species is 3 bp, corresponding to an amino acid in variable internal loop I4, and (v) there was no significant base frequency heterogeneity among individuals within species, nor between species ($G = 0.148$, d.f. = 3, $P < 0.0001$).

Tajima's D and Fu's F_s tests did not detect significant departures from neutrality in either species ($P > 0.10$). Of 33 total substitutions within *A. lucasi*, 29 were synonymous and 4 replacement [haplotypes S (site 8), Q, R, S (site 74), P (site 78) and J (site 323)], whereas all 22 substitutions within *C. coerulea* were synonymous.

Strong contemporary population structure, more fine scale in A. lucasi

Most (65/72) logs contained only a single *A. lucasi* haplotype. However, two or three haplotypes were sampled from seven logs, five in northern Tallaganda (Fig. 1c, Appendix I). *A. lucasi* appear to be scarce in BR: only three were collected despite substantial effort, but each possessed a unique mtDNA haplotype. Most (59/69) collecting sites of *C. caenoplana* also yielded single haplotypes. Ten logs yielded two to four haplotypes (Fig. 1c, Appendix I), not concentrated in any region of Tallaganda. In all cases, collection sites with two or more haplotypes contained representatives of the common regional haplotype. Both species displayed substantial genetic localization in mtDNA haplotype frequencies. This was stronger for *A. lucasi*, which was positively spatially autocorrelated at 0–10 km ($P < 0.01$), but significantly negatively autocorrelated in the 11–20 km bin ($P < 0.001$), for which *C. coerulea* was still positively autocorrelated ($P < 0.01$). Both were significantly negatively autocorrelated at 21–30 km ($P < 0.0001$) and for at least the next four bins.

Discrete allopatric genetic lineages in the two species, with northern region distinct

Artioposthia lucasi. For 197 individuals there were 32 polymorphic sites (24 parsimony informative), comprising 19 haplotypes. Maximum uncorrected sequence divergence was 4.9% compared to > 7.1% from outgroups. The TIM + I was the best-fit model of sequence evolution. The following parameters of GTR + I, estimated by PAUP* from one of the maximum-parsimony trees were used as initial parameters for the maximum-likelihood search: six substitution types (0.64, 3.98, 0.06, 0, 4.94 and 1), proportion of invariant sites (I) = 0.832**.** The first two maximum-likelihood iterations converged on the estimates of parameters (6 substitution types 0.96, 4.14, 0.06, 0, 5.15 and 1, and I = 0.829) and found the same tree (Fig. 2a). The tree shows deep phylogeographic structure. Four sequences found within south-central Tallaganda (T, S, Q and R) appear ancestral to the other haplotypes. The remaining sequences form lineages/groups with nonoverlapping ranges in northern, central, south-central and southern regions, except haplotype D, from a central Tallaganda group even though it occurred in two south-central individuals (Figs 1c and 2a). Because allopatric distribution of the clusters is likely a result of different evolutionary histories, some analyses were performed on the following five lineages (or pairs): south-central (haplotypes TS), south-central (QR), southern (GHI), central (ABCD + EF), and northern (JK + MNOP). Three of these lineages possessed high-frequency haplotypes, and 6 out of 10 unique haplotypes occurred in southern and south-central Tallaganda (Figs 1c and 2a, 3). The molecular clock hypothesis was rejected (–ln L without molecular clock enforced 855.34, –ln L with clock enforced 907.56, d.f. = 18, $P = 3.4*10^{-14}$).

Caenoplana coerulea. For 192 samples, of the 20 polymorphic sites, 13 were parsimony informative, representing 17 haplotypes. Maximum uncorrected divergence between any pair of *C. coerulea* haplotypes was 2.5% and divergence from outgroups was > 7.5%. TrN + I was the best-fit model of sequence evolution. The following parameters of GTR + I, estimated by PAUP* from one of the maximum-parsimony trees, were used as initial parameters for the maximum-likelihood search: six substitution types (3.4, 4.3, 1.7, 0, 8 and 1) and proportion of invariant sites (I) of 0.826. Five successive maximum-likelihood iterations with parameter re-estimation were needed before the same tree (Fig. 2b) was obtained and parameters converged on 6 substitution types (5.7, 3.9, 1.4, 0, 11.2 and 1) and I = 0.828. This tree was structured geographically, although the ranges of some clades overlapped (Fig. 2b). Two haplotypes from central Tallaganda (q and p) were apparently ancestral to the other haplotypes. The remaining haplotypes form four genetic lineages with allopatric distributions, analysed below: northern (haplotypes klmno), central (efghi), south-central (abcd) and southern (j). As with *A. lucasi*, several lineages possessed high frequency haplotypes, and the five unique ones were not concentrated in any part of the sampled area (Figs 1d and 2b). A molecular clock was rejected (–ln L without molecular clock enforced 734.8, –ln L with clock enforced 771.22, d.f. = 16, $P = 3.2 * 10^{-9}$).

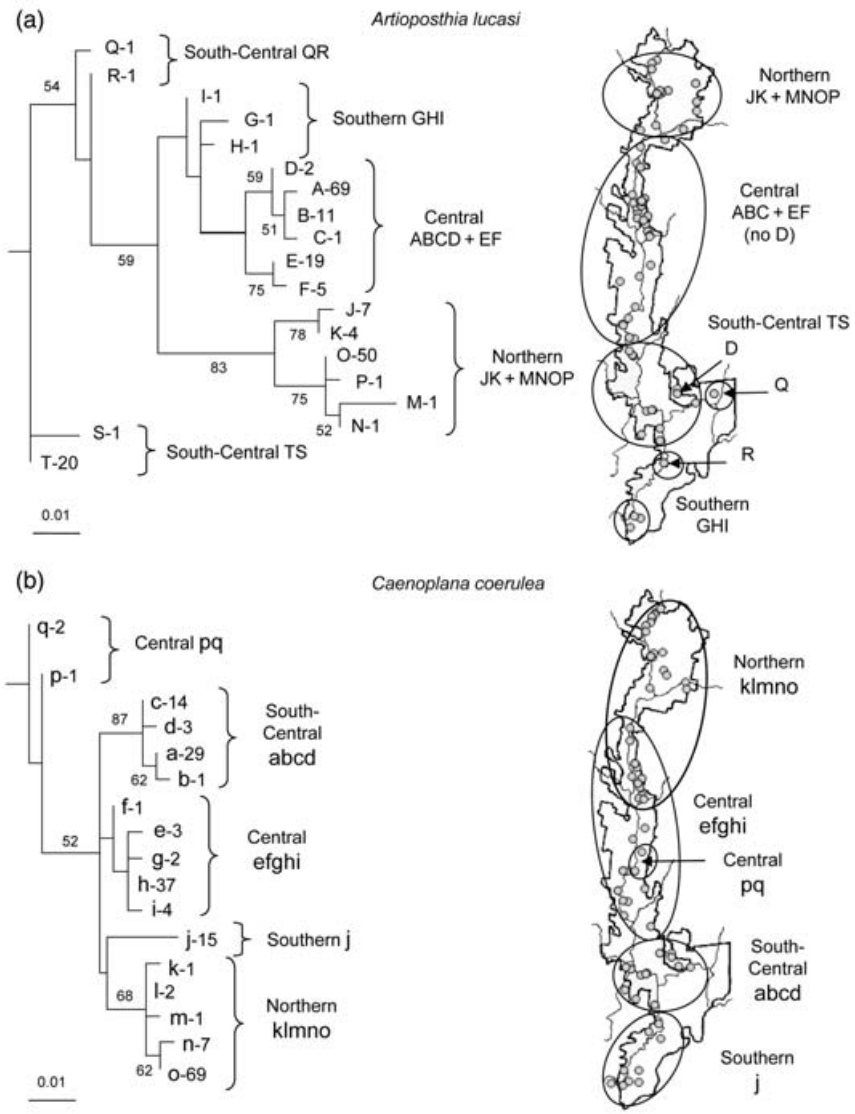

Fig. 2 Maximum-likelihood (ML) trees for (a) 19 unique mtDNA haplotypes (A–T) of *Artioposthia lucasi* and (b) 17 unique mtDNA haplotypes (a–q) of *Caenoplana coerulea*, rooted with outgroups, and geographic distribution of genetic lineages. Numbers after haplotypes indicate the total number of individuals sharing the same haplotype, brackets indicate genetic lineages, numbers by the branches indicate percentages of 100 ML bootstrap replicates (for *C. coerulea*, the clade comprising haplotypes q and p received 56% bootstrap support but was not recovered by the best ML tree). Ovals on maps show geographic distribution of genetic lineages; grey dots indicate sampling localities (logs).

Thus, both species show strong phylogeographic structuring, with well-diverged mtDNA lineages localized, with very few exceptions, to regions of 10 or a few tens of kilometres of latitude (Fig. 2).

Furthermore, in both species a distinct lineage is present in the north, suggesting a long history of isolation of northern Tallaganda from other regions, notably within *A. lucasi*.

Genetic diversity and variability of lineage-based genetic populations

Overall haplotype diversity (*h*) for *A. lucasi* was 0.79 (Table 1). Ignoring samples $N < 4$, *h* was moderate in the north (JK + MNOP), relatively high in central (ABCD + EF), and relatively low in south-central. For *C. coerulea*, overall *h* was similar (0.80), but in a different pattern: *h* increased from north, through central, to south-central (and was zero in the south, for which there are too few samples in *A. lucasi*). Nucleotide diversity (π) mirrored these geographic patterns (Table 1). Overall π was high in *A. lucasi* (0.025), while in *C. coerulea*, it was about half (0.012). Estimates of effective population size θ(S) within species were highest in northern JK + MNOP of *A. lucasi* and in central efghi of *C. coerulea* (Table 1).

Dynamics of lineage-based genetic populations: C. coerulea *growing*, A. lucasi *not*

Demographic analyses were performed for only northern (lineages JK + MNOP in *A. lucasi* and klmno in *C. coerulea*), central (ABCD + EF in *A. lucasi* and efghi in *C. coerulea*) and

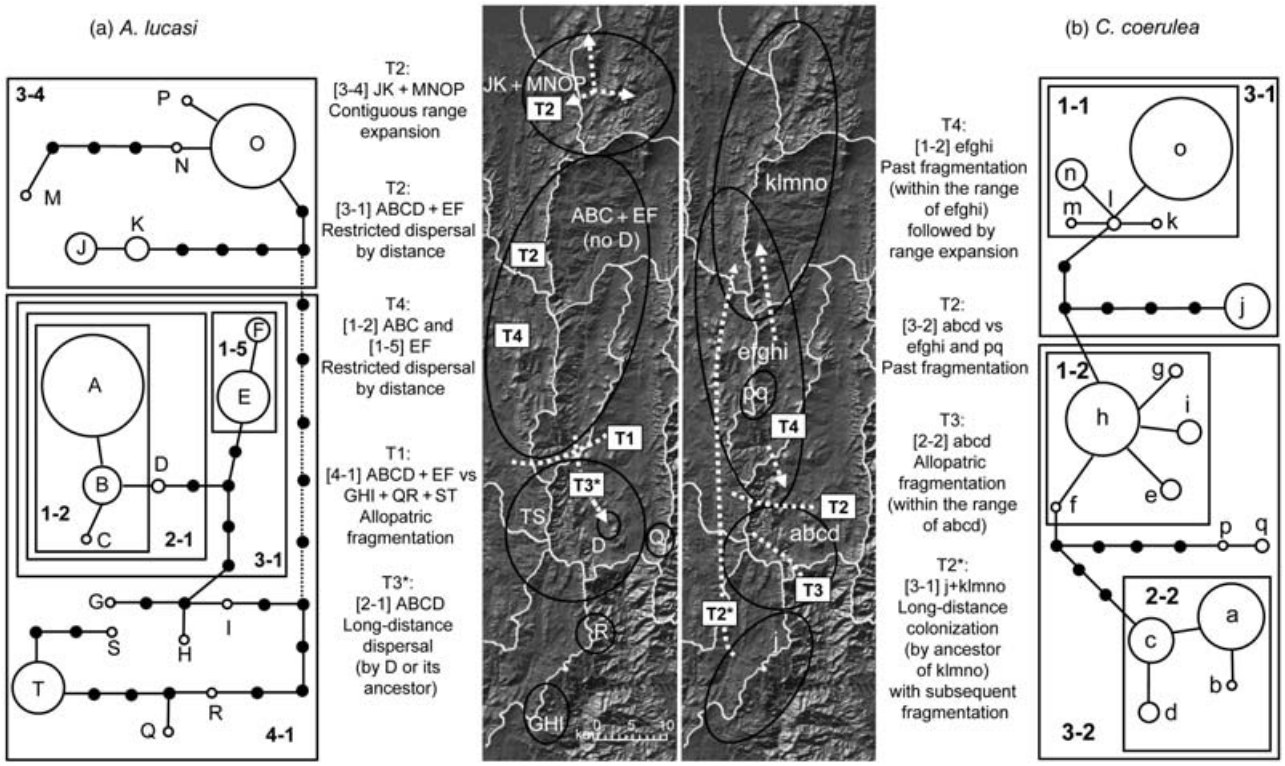

Fig. 3 Maps: evolutionary inferences suggested by nested clade analysis (NCA; Table 4) for (a) *Artioposthia lucasi* and (b) *Caenoplana coerulea*. T1–T4 boxes indicate relative timing of events as inferred from nesting level of the clades (T1, 4-step clade; T2, 3-step clade; T3, 2-step clade; T4, 1-step clade). Clades significant according to NCA are labelled in brackets as in Table 4 and Fig. 2. Black ellipses show simplified outlines of the clades' ranges (as on Fig. 2), dotted lines show historic fragmentation, and dotted arrows indicate direction of inferred dispersal. Asterisks indicate inferences which we consider unlikely given extremely low mobility of the flatworms (Discussion).
Networks: haplotype networks for (a) *A. lucasi* and (b) *C. coerulea* haplotypes estimated using statistical parsimony (loops resolved based on the maximum-likelihood trees, Fig. 2). Open circles indicate sampled haplotypes (Fig. 1), areas of the circles are proportional to number of individuals sharing the same haplotype, black circles indicate missing haplotypes. Dotted lines on *A. lucasi* network indicate connection between two networks found by TCS after confidence was relaxed to 92%. Significant nested clades found by NCA are identified by boxes and labelled as in Table 4.

Table 1 Genetic characteristics of lineage-based genetic populations (see Fig. 2)

Species	Genetic population	No. of individuals	No. of haplotypes	Haplotype diversity (*h*)	SD (*h*)	Nucleotide diversity (π)	SD (π)	θ (S)	SD (θ (S))
A. lucasi	South-central TS	21	2	0.095	0.084	0.0008	0.001	0.834	0.532
	South-central QR	2	2	1		0.0055	0.0067	2.0	1.732
	Southern GHI	3	3	1	0.27	0.0073	0.0065	2.667	1.919
	Central ABCD	83	4	0.294	0.06	0.001	0.0011	0.601	0.368
	Central EF	24	2	0.344	0.099	0.0009	0.0011	0.268	0.268
	Central ABCD + EF	107	6	0.545	0.05	0.0065	0.0039	1.525	0.636
	Northern JK	11	2	0.509	0.101	0.0014	0.0014	0.341	0.341
	Northern MNOP	53	4	0.111	0.059	0.0007	0.0009	1.322	0.631
	Northern JK + MNOP	64	6	0.379	0.07	0.0059	0.0037	2.749	1.027
C. coerulea	Central pq	3	2	0.667	0.314	0.0018	0.0023	0.667	0.667
	South-central abcd	47	4	0.538	0.058	0.0018	0.0016	0.679	0.421
	Central efghi	47	5	0.375	0.087	0.0011	0.0012	0.906	0.502
	Southern j	15	1	0	0	0	0	0	0
	Northern klmno	80	5	0.251	0.062	0.0008	0.001	0.606	0.371

Table 2 Tests for demographic expansion and population growth rate estimates for lineage-based genetic populations. Models of demographic (MDE) and spatial (MSE) population expansion were estimated in ARLEQUIN. Parameters of MDE: τ, relative time since population expansion; θ_0 and θ_1 are relative population sizes before and after expansion. Parameters of MSE: τ, relative time since spatial expansion; θ, effective size of each deme; and *M*, relative rate of gene exchange among demes. NS, not significant at $P < 0.05$; none, ARLEQUIN failed to fit the model; NE, not estimated. FLUCTUATE: θ_{NG} = a composite measure of effective population size and the per-site neutral mutation rate ($2N_e\mu$) estimated under assumption of no growth, $\theta_G = \theta$ estimated under the model of growing population; g, exponential rate of population growth, standard deviation of the mean of five replicates are shown in parentheses, asterisk indicates significance (*sensu* Lessa *et al*. 2003; see Methods). Positive values of g suggest population growth, negative values = population decline

				Model of demographic expansion				Model of spatial expansion				FLUCTUATE		
Species	Genetic population	Fu's F_s	R_2	MDE test	τ	θ_0	θ_1	MSE test	τ	θ	*M*	θ_{NG}	θ_G	g
A. lucasi	South-central (TS)	0.49 NS	0.21 NS	$P = 0.02$	3	0.05	0.06	NS	3.49	0	0.123	—	—	—
	Central (ABCD + EF)	2.96 NS	0.15 NS	NS	6.98	0	1.16	NS	6.23	0.55	0.717	0.0036 (0.0005)	0.0031 (0.0004)	−147.47* (20.72)
	Northern (JK + MNOP)	1.77 NS	0.09 NS	NS	3	0.43	0.43	NS	6.63	0.13	0.509	0.0069 (0.0006)	0.0056 (0.0002)	−58.03* (9.18)
C. coerulea	South-central (abcd)	−0.31 NS	0.11 NS	none	NE	NE	NE	none	NE	NE	NE	0.0020 (0.0002)	0.0025 (0.0004)	798.21 (308.8)
	Central (efghi)	−2.64 $P = 0.03$	0.06 $P = 0.08$	none	NE	NE	NE	none	NE	NE	NE	0.0030 (0.0001)	0.0075 (0.0018)	3559.8* (851.89)
	Northern (klmno)	−3.11 $P = 0.02$	0.07 NS	NS	3	0	0.34	NS	0.25	0.194	2.089	0.0023 (0.0006)	0.0051 (0.0021)	3289.25 (1183.59)

south-central (TS in *A. lucasi* and abcd in *C. coerulea*; Table 2), thus we further omit specifications of lineages in this section.

Populations of *A. lucasi* appear to be declining or, at least, not expanding. Neither Fu's F_s nor R_2 detected population growth, the model of demographic expansion (MDE) was rejected for south-central (Table 2), and northern and central populations had bimodal mismatch distributions (two sublineages each, data not shown). The model of spatial expansion (MSE) was not rejected for any population, but large values of τ suggest that spatial expansion may have occurred relatively long ago. Significantly negative values of g for northern and central lineages suggested that these populations are declining (south-central had only two haplotypes).

In contrast, the same tests pointed to population growth/departure from neutral evolution in *C. coerulea*. All Fu's F_s were negative (significantly so for two lineages), although R_2 did not detect any growth (central population marginally significant). ARLEQUIN could not fit MDE and MSE to central and south-central populations, but mismatch distributions were unimodal for all populations (data not shown) consistent with growth. Neither MDE nor MSE was rejected for the northern population, for which moderate τ (MDE) suggests that demographic expansion occurred some time ago, whereas small τ (MSE) indicates recent spatial expansion. Values of g (population growth) were positive for all populations (significant for central) (Table 2).

Genetic characteristics of (sub)catchment-based regions and limited gene flow among them

Haplotype diversity (*h*) within (sub)catchment-based regions of *A. lucasi* ranged by an order of magnitude, excluding zero values (Table 3). For *C. coerulea*, *h* was more consistent, but nonzero values still varied fivefold. Nucleotide diversity (π) was also more variable among *A. lucasi* than *C. coerulea* regions (Table 3). The maximum number of haplotypes per region was found in central and northern regions: ML + HCR and ESR-Ba (five haplotypes) for *A. lucasi*, and in ESR-AR (six) and ML + HCR (five) in *C. coerulea* (Table 3).

Analyses of molecular variance indicated strong regional differentiation: > 75% of all variance in haplotype frequency and molecular divergence in both species was explained by organization into 12 (sub)catchment-based regions ($P < 0.001$). Most pairwise φ_{ST} values were large and significant (Appendices IV and V) indicating long-term historical isolation and extremely low gene flow between regions. Relatively small values of pairwise φ_{ST} (0–0.2) were observed for some neighbouring regions in south-central and southern Tallaganda for *A. lucasi* and in central and southern Tallaganda for *C. coerulea* (Appendix III) indicating the possibility of recent or contemporary gene flow between these regions.

A plot of pairwise region comparisons for two species (Fig. 4) shows the significant positive relationship expected if the species responded similarly to historic fragmentation

Table 3 Sampling statistics and genetic characteristics of (sub)catchment-based microgeographic regions and their boundaries. Numbers after haplotypes (Fig. 2) indicate the number of individuals sharing the same haplotype. Abbreviations for the regions are given in Methods and in the legend for Fig. 1. MO + HCR includes MO, MO-HCR and HCR samples, ESR-AR includes AR samples

Species	Region	No. of individuals	No. of logs	No. of haplotypes haplotypes	Haplotype diversity (*h*)	SD (*h*)	Nucleotide diversity (π)	SD (π)	Distribution of haplotypes within regions
A. lucasi	HCR-LG	31	3	2	0.065	0.059	0.0002	0.0004	O30, P1
	MO + HCR	32	11	5	0.601	0.079	0.0097	0.0056	J7, K4, M1, N1, O19
	ESR-MO	24	7	3	0.54	0.062	0.0086	0.0051	A14, E9, F1
	ESR-Ba	63	25	5	0.236	0.070	0.0046	0.003	A55, B1, E2, F4, O1
	ESR-Je	6	3	1	0	0	0	0	B6
	ESR-AR	23	9	4	0.688	0.055	0.0185	0.01	B4, C1, E8, T10
	PSR	6	3	2	0.533	0.172	0.0161	0.0104	D2, T4
	PSR-DU	1	1	1	NA		NA		Q1
	PSR-NU	4	3	1	0	0	0	0	T4
	NU	1	1	1	NA		NA		S1
	NU-BR	3	3	2	0.667	0.314	0.0073	0.0066	R1, T2
	BR	3	3	3	1	0.272	0.0073	0.0066	G1, H1, I1
	Total	197	72	19					
C. coerulea	HCR-LG	31	8	3	0.127	0.08	0.0004	0.0006	l1, n1, o29
	MO + HCR	39	8	5	0.323	0.093	0.0012	0.0012	k1, l1, m1, n4, o32
	ESR-MO	4	3	3	0.667	0.204	0.0074	0.0059	h2, o2
	ESR-Ba	30	13	4	0.563	0.088	0.0051	0.0033	e3, h19, n2, o6
	ESR-Je	7	5	3	0.524	0.209	0.0047	0.0036	g1, h5, q1
	ESR-AR	16	8	6	0.542	0.147	0.0058	0.0038	c1, f1, g1, h11, p1, q1
	PSR	23	6	4	0.629	0.084	0.0062	0.004	a5, c13, d1, i4
	PSR-NU	16	4	2	0.125	0.106	0.0007	0.0009	a15, d1
	NU	7	3	2	0.286	0.196	0.0071	0.005	a6, j1
	NU-BR	9	5	3	0.417	0.191	0.0093	0.006	a1, d1, j7
	BR	7	4	1	0	0	0	0	j7
	NU-BO	3	2	2	0.667	0.314	0.0018	0.0023	b1, a2
	Total	192	69	17					

($R^2 = 0.3$, $P < 0.001$), but also highlights the differences in genetic structure. For several between-region comparisons, high gene flow in *A. lucasi* occurred where it was restricted in *C. coerulea* (cloud of points B on Fig. 4, all involving the same small area of topographic complexity in south-central Tallaganda where three catchments meet), whereas for two comparisons, relative gene flow was the converse (two points, C on Fig. 4). Three comparisons between neighbouring regions (stars, Fig. 4) yielded high ϕ_{ST} values in both species, indicating historic vicariant events, i.e. isolation of northern Tallaganda from the rest, and isolation of central Tallaganda from south-central (Appendix III).

Nested clade analyses

Two disconnected networks of *A. lucasi* haplotypes were obtained with 95% confidence in TCS: one comprised haplotypes localized in northern Tallaganda, whereas the other included the remaining haplotypes (Fig. 2). The two networks connected at 92% confidence. A single loop was resolved using the maximum-likelihood phylogeny (Fig. 2a). Six clades were significant under NCA, five of which were also seen in maximum-likelihood analysis (Table 4). Inferred processes/events were old allopatric fragmentation between central and south-central Tallaganda, medium-age contiguous range expansion within the northern region, and medium plus young restricted dispersal by distance in central lineages (clades and map locations in Fig. 3a). Finally, the disjunct, restricted distribution of haplotype D outside the range of its closest relatives led to the inference of moderately recent long-distance dispersal of haplotype D (or an ancestor) from central to south-central Tallaganda.

A single network was obtained for *C. coerulea* haplotypes with 95% confidence (Fig. 2), five loops requiring resolution. Five clades were significant by NCA (two supported by maximum-likelihood analysis) (Table 4). NCA inferred moderately old long-distance colonization of southern Tallaganda from the north, with subsequent fragmentation between them (Fig. 3b), past fragmentation between central and south-central Tallaganda, moderately recent allopatric east–west fragmentation in south-central Tallaganda, and recent fragmentation in central Tallaganda followed by range expansion.

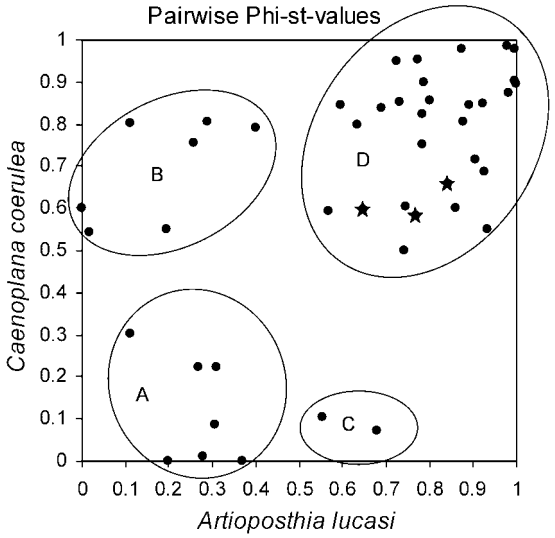

Fig. 4 Comparison of pairwise φ_{ST} values (Appendices IV and V) for *Artioposthia lucasi* (*x*-axis) and *Caenoplana coerulea* (*y*-axis). Ellipses indicate clouds of points corresponding to (a) presence of recent and/or contemporary gene flow in both species all involving samples near subcatchment watersheds (includes comparisons between PSR/PSR-NU, ESR-MO/ESR-Ba, ESR-MO/ESR-Je, ESR-MO/ESR-AR, ESR-Ba/ESR-Je, HCR-LG/MO+HCR, ESR-Je/ESR-AR); (b) presence of recent gene flow in *A. lucasi* with historic isolation in *C. coerulea* all involving the same area of high, localized watershed complexity in the south-central area (PSR/NU-BR, ESR-AR/PSR, PSR-NU/NU-BR, ESR-AR/NU-BR, ESR-AR/BR, ESR-AR/PSR-NU, PSR/BR); (c) historical isolation within *A. lucasi* with recent gene flow within *C. coerulea* (ESR-Ba/ESR-AR, NU-BR/BR); and (d) long-term historical isolation in both species (includes comparisons between non-neighbouring regions and three instances of isolation between neighbouring regions, denoted by stars: MO+HCR/ESR-MO, MO+HCR/ESR-Ba, and ESR-Je/PSR; these three lie at the greatest regional breaks).

Discussion

Evolutionary history of Tallaganda flatworms

Pliocene drying, long cycles of wet–dry in the early to mid-Pleistocene and intense high amplitude cycles in the late Pleistocene are thought to have had a major impact on distribution and genetic structure within the Tallaganda model system (Garrick *et al.* 2004). The presence of ancestral haplotypes, congruent and highly structured geographical lineages and the occurrence of several genetic lineages within regions (Fig. 2) suggest long-term persistence of both flatworm species. Remarkably similar geographic clustering of haplotypes closely matches major catchments, and the presence of substantial, localized genetic diversity within major catchments in Tallaganda suggests that these regions were not completely deforested during cold and dry Pleistocene periods. Ancestral haplotypes of both species appear in south-central (TS and QR in *Artioposthia lucasi*) and central (pq in *Caenoplana coerulea*) Tallaganda, indicating that PSR and ESR represent historically refugial environments (Figs 1 and 2). Thus, it seems that both flatworms inhabited Tallaganda prior to late Pleistocene forest fragmentation, and phylogeographic structure observed today reflects many evolutionary events, including multiple contractions and expansions of the ranges, historic fragmentation and gene flow. Several presumably simultaneous vicariant events (likely caused by major retraction of Pleistocene forest) seem to have split the range of widespread ancestral populations of *A. lucasi* and *C. coerulea* into northern, central, south-central and southern groups. Unresolved relationships among major *C. coerulea* lineages (Fig. 2b) indicated that this species probably was not very subdivided prior to vicariance compared to *A. lucasi* (Fig. 2a).

Table 4 Population historical inferences (presented in chronological order) suggested by nested clade analysis. Results presented only for the clades with significant association between haplotype and geography ($P < 0.05$). See also Fig. 3

Species	Clade	Haplotypes	Permutation *P* value	Chain of inference	Biogeographic inference
A. lucasi	4-1	(ABCD + EF) + (GHI + QR + ST)	< 0.0001	1-19	Allopatric fragmentation
	3-1	ABCD + EF	< 0.0001	1-2-3-4	Restricted dispersal by distance
	34	JK + MNOP	0.0080	1-2-11-12	Contiguous range expansion
	2-1	ABCD	0.0250	1-19-20-2-11-12-13-21	Long-distance movement
	1-2	ABC	< 0.0001	1-2-3-4	Restricted dispersal by distance
	1-5	EF	< 0.0001	1-2-3-4	Restricted dispersal by distance
C. coerulea	3-1	j + klmno	< 0.0001	1-19-20-2-11-12–13	Long-distance colonization coupled with subsequent fragmentation
	3-2	abcd + efghi	< 0.0001	1-2-3-5-15	Past fragmentation
	2-2	abcd	< 0.0001	1-19	Allopatric fragmentation
	1-1	klmno	< 0.0001	1-2-11-17	Inconclusive outcome
	1-2	efghi	< 0.0001	1-2-3-5-6-13	Past fragmentation followed by range expansion

Whereas *C. coerulea* displays its highest diversity (*h* and π) in central and south-central Tallaganda, *A. lucasi* shows its highest diversity in the central and northern regions (Table 1). A single haplotype in 15 *C. coerulea* in southern Tallaganda suggests a strong bottleneck there, in contrast to *A. lucasi* for which the three samples were all unique. Genetic diversity in both species is high in central Tallaganda (ESR), as predicted by the *a priori* phylogeographic model (Garrick *et al*. 2004). Although haplotype diversity was comparable in the two species, nucleotide diversity in *A. lucasi* was twice that of *C. coerulea* and effective population size estimates (θ in Table 1, θ_{NG} in Table 2) were consistently larger, suggesting that *A. lucasi* species has a longer history of continuous occupation of Tallaganda, or at least its stronger population substructure has helped to retain older haplotypes. The persistence of relatively deeply ramified diversity in *A. lucasi* in the face of climate change and forest contraction suggests the testable assertion that this species must have greater ability than *C. coerulea* to resist intense and sustained cool, dry conditions in small habitat patches. Coalescence analyses indicate population decline within *A. lucasi* in contrast to growth in *C. coerulea*, which might reflect relatively adverse responses of *A. lucasi* to Holocene climate warming (so explaining the difficulty of sampling *A. lucasi* in the south, the lowest-altitude sampled area) but may be an artefact of the effect of strong population subdivision on retention of older haplotypes.

Although essentially all of Tallaganda is currently forested and the present flatworms are widespread, spatial autocorrelation and haplotypic distributions indicate ongoing genetic subdivision. This can lead to deep genetic divergence if reiterated (Chenoweth & Hughes 2003; Hewitt 2004a, b). It appears that the frequency of the climate cycles, short duration of interglacial conditions during the Pleistocene (Hope 1994; Hewitt *et al*. 2004) and perhaps local adaptation, have resulted in limited gene flow in both species, even at the interfaces between many closely adjacent regions (Figs 1 and 2, Appendix III).

Timing of evolutionary events and pre-Pleistocene history of Tallaganda

Of commonly employed DNA regions, COI provides the most consistent rate of evolution between different lineages of insects (Gaunt & Miles 2002). Estimates of substitution rates range from ~1.7% to 2.3% per million years (details in Garrick *et al*. 2004). However, mutation rates calculated from pedigrees and short timescales can be much higher (Ho *et al*. 2005; Penny 2005), raising questions about the validity of recent/intraspecific comparisons of the sorts of rates cited above. Much of that extra short-term variation appears due to slightly deleterious mutations not yet removed by selection, so will be more problematic in species with low effective population size and, thus, weaker potential for purifying selection (stronger genetic drift). Rejection of molecular clock in both flatworm species (likely caused by retained ancestral haplotypes) preclude us from confidently estimating ages of splitting events. Nonetheless, given that ancestral (by outgroup rooting) haplotypes T for *A. lucasi* and q for *C. coerulea* (Fig. 2) are 4.9% and 2.5% different from the most distant haplotypes, if we apply standard rates of mtDNA substitution with the usual attendant caveats, evolution of these haplotypes (and thus history of the contemporary genetic diversity within Tallaganda) might have started in the late Pliocene for *A. lucasi* and in the Pleistocene for *C. coerulea*.

Under the scenarios outlined above, and by analogy with patterns seen in 'giant' Collembola in the same region (Garrick *et al*. 2004), we postulate that a few *A. lucasi* haplotypes survived a relatively early drying event (putative ancestral sequences in Fig. 2a), while the same event left no traces of *C. coerulea*, if previously present. Perhaps during the Pleistocene, *A. lucasi* could have spread over Tallaganda, at the same time as *C. coerulea* colonized Tallaganda via the central (ESR) region (Fig. 2b). Through the Pleistocene, both species probably completed colonization of Tallaganda and *A. lucasi* experienced considerable local differentiation. Historical isolation of northern, central and southern lineages in *A. lucasi* and northern, south-central abcd, central and southern lineages within *C. coerulea* (Fig. 2) was probably caused by one or several sequential cycles of drying and cooling in the Pleistocene. These suggestions could be further investigated by application of mtDNA sequence data from additional gene regions, more sampling of close outgroups so allowing application of M–K tests, and nuclear sequence data.

NCA inferences in comparison to those from other approaches

Although NCA offers a unique opportunity to suggest evolutionary events from spatial distribution of the haplotypes and their relatedness, its inability to compare alternative hypotheses quantitatively has been criticized (Knowles & Maddison 2002). In the present study, the two inferences of long-distance dispersal appear biologically unlikely. In the case of the apparent dispersal of haplotype *D* (or ancestor) of *A. lucasi*, dispersal may have occurred along the eastern fringe of Tallaganda, where suitable habitat and flatworms have been extinguished by natural and human agents. A relatively old long-distance colonization [of northern Tallaganda (HCR) from the far south (BR)] was inferred by NCA for *C. coerulea*. Given low mobility of flatworms, absence of haplotypes related to j + klmno in central Tallaganda, and poor bootstrap support for the ML sister-clade relationships, this long-distance colonization seems less likely than a vicariance explanation. Vicariance was supported by the genetic patterns in

A. lucasi, and also by patterns within other lineages of *C. coerulea* itself, including the congruent splits between central and south-central Tallaganda. Nonetheless, NCA highlighted several important inferences supported by other analyses, including fragmentation of central vs. south-central Tallaganda in both species, restricted dispersal by distance within central *A. lucasi*, and contiguous range expansion in the northern population of *A. lucasi*. The NCA inference of past fragmentation in central Tallaganda *C. coerulea* followed by range expansion was not supported by φ_{ST} analysis, but is plausible and consistent with haplotype distributions. Finally, the inferred allopatric fragmentation in the south-central population of *C. coerulea* was detected also by φ_{ST} analysis.

Potential impacts of using only mtDNA, and natural selection, on demographic inferences

There are well-known limitations to using mtDNA alone in phylogeography — in particular, it is preferable to have nuclear markers (Ballard & Whitlock 2004). However, nuclear marker development has proven difficult for these species. Set against a multitaxon phylogeographic model comprising multiple regions, we consider the mtDNA data here substantial and informative in a paired comparison of two species. The hermaphroditic nature of the present organisms also makes it likely that mtDNA is a better reflector of organismal patterns than in bisexual organisms, which can have strong sex-biased genetic patterns.

Mitochondrial DNA may be subject to strong natural selection (Ballard & Whitlock 2004). While selective sweeps would tend to 'reset the clock' and cause underestimation of timing of divergences of populations, the data are not suggestive of this (e.g. there are starlike radiations within most regions in both species). Neither Fu's F_s nor Tajima's D detected selection for species level data. At the population level, Fu's F_s detected departure from neutrality for the central and northern *C. coerulea* lineages, which might have been caused by selection and/or population growth. Because growth was also suggested by FLUCTUATE results, not only for these two populations but also for south-central *C. coerulea*, we believe that population growth caused significance in Fu's F_s.

Local and general implications for landscape management

Garrick *et al*. (2004) proposed that the ESR should contain the greatest number of high-quality refuges from cool, dry conditions for saproxylic invertebrates, and outlined the Tallaganda model for testing geographic congruence among diverse taxa. For *A. lucasi*, ESR, PSR and HCR all showed evidence of multiple distinct refuges in each region, although the boundary of PSR appears to be relatively permeable to migration (e.g. Fig. 4). The high diversity at BR despite apparently low densities could also reflect multiple refuges; alternatively it might be explained by dispersal from the Great Dividing Range. Colonization of the other regions from outside Tallaganda is unlikely given its strong physical and ecological isolation (Garrick *et al*. 2004), consistent with the distinctiveness for both species in the northern (most isolated) region, HCR. For *C. coerulea*, ESR seems much more clearly to have been the most important refuge at Tallaganda and potentially the source of the species throughout: this region contains two of five genetically distinct haplotype groups and its sequences are the most strongly represented at the centre of the network, supported to be ancestral by maximum-likelihood analysis (Fig. 2).

The main aspect of the data for both species that was not predicted from the *a priori* physical model for Tallaganda was the high level of mtDNA haplotype diversity, relatively deep divergences and distinctiveness at HCR, where long-term refuges are implied. The main reason that ESR was identified as a strong refuge area is its east-facing aspect and > 15 east-facing deep creeks, which, via coastal influences, are proposed to have ameliorated climatic change and allowed pockets of forest to persist (Garrick *et al*. 2004). HCR contains a major east-facing drainage, which may explain its apparent effectiveness as a refuge.

The patterns we have analysed for two ecologically different flatworms are in many ways very similar to those reported for slime-mould-grazing Collembola at Tallaganda (Garrick *et al*. 2004; Garrick & Sunnucks 2006). While the estimated order and intensities of splits among regions differ from species to species, the congruence in locations of genetic populations is strong, and largely predicted by catchments. The ability of Tallaganda to hold deeply diverged mtDNA sequences in a fauna dependent on cool and moist conditions suggests that the negative effects of vegetation contraction can be moderated for these kinds of organisms by the presence of small refuges, and/or that changes in temperature and/or altitudinal change in the tree line over the last few million years have been much less extreme than generally supposed.

The maintenance of genetic diversity and the potential for organisms to adapt locally and evolve is of major concern in evolutionary and conservation biology (Frankham *et al*. 2002). The grain (relevant spatial scale) of environment at which the saproxylic ecological community operates, and the diversity of microhabitats offered by the complex topography of Tallaganda appear to have interacted to provide a Southern Hemisphere temperate example of the importance of the interaction of life history and palaeoclimatic impacts envisaged for other ecological regions (Hewitt 2004a, b). We propose that similar patterns are likely to apply to relatively immobile, moisture-dependent organisms, and that catchment-based units will often provide a rational basis for management consideration and research.

Acknowledgements

We thank Leigh Winsor for flatworm information, field volunteers and our research groups, in particular Melanie Lancaster. Luciano Beheregaray and Michael Turelli gave useful advice and comments. Bob Mesibov continues to be a welcome source of challenging, interesting ideas. The manuscript was improved by comments of an anonymous reviewer and Graham Wallis. Samples were collected under permits from New South Wales State Forests and National Parks. Funding included ARC DP0211156 and Genetics Society of Australia Summer Studentship to S.C. The computer cluster used to estimate ML phylogenies and run FLUCTUATE was funded by National Science Foundation DGE-0114387 to DM Hillis.

References

Avise JC & Walker D (1998) Pleistocene phylogeographic effects on avian populations and the speciation process. *Proceedings of the Royal Society of London. Series B, Biological Sciences*, **265**, 457–463.

Ayoub NA, Riechert SE (2004) Molecular evidence for Pleistocene glacial cycles driving diversification of a North American desert spider, *Agelenopsis aperta*. *Molecular Ecology*, **13**, 3453–3465.

Ballard JWO, Whitlock MC (2004) The incomplete natural history of mitochondria. *Molecular Ecology*, **13**, 729–744.

Barclay S, Ash JE, Rowell DM (2000a) Environmental factors influencing the presence and abundance of a log-dwelling invertebrate, *Euperipatoides rowelli* (Onychophora: Peripatopsidae). *Journal of the Zoological Society of London*, **250**, 425–436.

Barclay SD, Rowell DM, Ash JE (2000b) Pheromonally-mediated colonization patterns in the velvet worm *Euperipatoides rowelli* (Onychophora). *Journal of the Zoological Society of London*, **250**, 437–446.

Beavis AS, Rowell DM (2006) Phylogeography of two Australian species of funnel web spider (Arnaeae: Mygalomorphae: Hexathelidae: *Hadronyche & Atrax* in Tallaganda State Forest, New South Wales). In: *Insect Biodiversity and Dead Wood: Proceedings of a Symposium for the 22nd International Congress of Entomology. General Technical Report* (eds Grove SJ, Hanula JL), pp. 23–29. US Department of Agriculture Forest Service, Southern Research Station, Asheville, North Carolina.

Chenoweth SF, Hughes JM (2003) Speciation and phylogeography in *Caridina indistincta*, a complex of freshwater shrimps from Australian heathland streams. *Marine and Freshwater Research*, **54**, 807–812.

Clement M, Posada D, Crandall KA (2000) TCS: a computer program to estimate gene genealogies. *Molecular Ecology*, **9**, 1657–1660.

Cooper SJB, Hinze S, Leys R, Watts CHS, Humphreys WF (2002) Islands under the desert: molecular systematics and evolutionary origins of stygobitic water beetles (Coleoptera: Dytiscidae) from central Western Austalia. *Invertebrate Systematics*, **16**, 589–598.

De Chaine EG, Martin AP (2004) Historical cycles of fragmentation and expansion in *Parnassius smintheus* inferred from mtDNA. *Evolution*, **58**, 113–127.

Dendy A (1891) On the Victorian land planarians. *Transactions of the Royal Society of Victoria*, **2**, 65–80.

Excoffier L, Smouse PE, Quattro JM (1992) Analysis of molecular variance inferred from metric distances among DNA haplotypes: application to human mitochondrial DNA restriction data. *Genetics*, **131**, 479–491.

Excoffier L, Laval G, Schneider S (2005) ARLEQUIN ver. 3.0: An integrated software package for population genetics data analysis. *Evolutionary Bioinformatics Online*, **1**, 47–50. http://cmpg.unibe.ch/software/arlequin3.

Eyre-Walker A (2002) Changing effective population size and the McDonald-Kreitman test. *Genetics*, **162**, 2017–2024.

Frankham R, Ballou JD, Briscoe DA (2002) *Introduction to Conservation Genetics*. Cambridge University Press, New York.

Fu YX (1997) Statistical tests of neutrality of mutations against population growth, hitchhiking and background selection. *Genetics*, **147**, 915–925.

Garrick RC, Sunnucks P (2006) Development and application of three-tiered nuclear DNA genetic markers for basal Hexapods using single-stranded conformation polymorphism coupled with targeted DNA sequencing. *BMC Genetics*, **7**, 11. http://www.biomedcentral.com/1471-2156/7/11.

Garrick RC, Sands CJ, Rowell DM, Tait NN, Greenslade P, Sunnucks P (2004) Phylogeography recapitulates topography: very fine-scale local endemism of a saproxylic 'giant' springtail at Tallaganda in the Great Dividing Range of south-east Australia. *Molecular Ecology*, **13**, 3329–3344.

Garrick RC, Sands CJ, Sunnucks P (2006) The use and application of phylogeography for invertebrate conservation research and planning. In: *Insect Biodiversity and Dead Wood: Proceedings of a Symposium for the 22nd International Congress of Entomology. General Technical Report* (eds Grove SJ, Hanula JL), pp. 15–22. US Department of Agriculture Forest Service, Southern Research Station, Asheville, North Carolina.

Gaunt MW, Miles MA (2002) An insect molecular clock dates the origin of the insects and accords with palaeontological and biogeographic landmarks. *Molecular Biology and Evolution*, **19**, 748–761.

Hewitt GM (2004a) A climate for colonization. *Heredity*, **92**, 1–2.

Hewitt GM (2004b) Genetic consequences of climatic oscillations in the Quaternary. *Philosophical Transactions of the Royal Society of London. Series B, Biological Sciences*, **359**, 183–195.

Hewitt G, McKinnon GW, Lascoux M, McKinnon GE (2004) Glacial refugia and reticulate evolution: the case of the Tasmanian eucalypts — Discussion *Philosophical Transactions of the Royal Society of London. Series B*, **359**, 284–284.

Ho S, Phillips MJ, Cooper A, Drumond AJ (2005) Time dependence of molecular rate estimation and systematic overestimation of recent divergence times. *Molecular Biology and Evolution*, **22**, 1561–1568.

Hope GS (1994) Quaternary vegetation. In: *History of the Australian Vegetation: Cretaceous to Recent*, pp. 368–389. Cambridge University Press, Cambridge, UK.

Hugall A, Moritz C, Moussalli A, Stanisic J (2002) Reconciling paleodistribution models and comparative phylogeography in the Wet Tropics rainforest land snail Gnarosophia bellendenkerensis (Brazier 1875). *Proceedings of the National Academy of Sciences, USA*, **99**, 6112–6117.

Knowles LL (2001) Did the Pleistocene glaciations promote divergence? Tests of explicit refugial models in montane grasshopprers. *Molecular Ecology*, **10**, 691–701.

Knowles LL, Maddison WP (2002) Statistical phylogeography. *Molecular Ecology*, **11**, 2623–2635.

Kuhner MK, Yamato J, Felsenstein J (1998) Maximum likelihood estimation of population growth rates based on the coalescent. *Genetics*, **149**, 429–434.

Lessa P, Cook JA, Patton JL (2003) Genetic footprints of demographic expansion in North America, but not Amazonia, during

the Late Quaternary. *Proceedings of National Academy of Science, USA*, **100**, 10331–10334.

Lunt DH, Zhang D-X, Szymura JM, Hewitt GM (1996) The insect cytochrome oxidase I gene: evolutionary patterns and conserved primers for phylogenetic studies. *Insect Molecular Biology*, **5**, 153–165.

McDonald JH, Kreitman M (1991) Adaptive protein evolution at the Adh locus in *Drosophila*. *Nature*, **351**, 652–654.

Moritz C, Richardson KS, Ferrier S *et al.* (2001) Biogeographic concordance and efficiency of taxon indicators for establishing conservation priority in a tropical rainforest biota. *Proceedings of the Royal Society of London. Series B, Biological Sciences*, **268**, 1875–1881.

Moseley HN (1877) Notes on the structure of several forms of land planarian with a description of two new genera and several new species, and a list of all species at present known. Quarterly. *Journal of Microscopical Science*, **17**, 273–292.

Nei M, Kumar S (2000) *Molecular Evolution and Phylogenetics*. Oxford University Press, New York.

Peakall R, Smouse PE (2001) GENALEX *V5: Genetic Analysis in Excel, Population Genetic Software for Teaching and Research*. Australian National University, Canberra, Australia.

Penny D (2005) Relativity for molecular clocks. *Nature*, **436**, 183–184.

Pfenninger M, Posada D (2002) Phylogeographic history of the land snail *Candidula unifasciata* (Helicellinae, Stylommatophora): fragmentation, corridor migration and secondary contact. *Evolution*, **56**, 1776–1788.

Posada D, Crandall KA (1998) Modeltest: testing the model of DNA substitution. *Bioinformatics*, **14**, 817–818.

Posada D, Crandall KA, Templeton AR (2000) GEODIS: a program for the cladistic nested analysis of the geographical distribution of genetic haplotypes. *Molecular Ecology*, **9**, 487–488.

Ramos-Onsins SE, Rozas J (2002) Statistical properties of new neutrality tests against population growth. *Molecular Biology and Evolution*, **19**, 2092–2100.

Rozas J, Sánchez DelBarrio JC, Messeguer X, Rozas R (2003) DNASP, DNA polymorphism analyses by the coalescent and other methods. *Bioinformatics*, **19**, 2496–2497.

Schauble CS, Moritz C (2001) Comparative phylogeography of two open forest frogs from eastern Australia. *Biological Journal of the Linnean Society*, **74**, 157–170.

Schneider S, Excoffier L (1999) Estimation of past demographic parameters from the distribution of pairwise differences when the mutation rates very among sites: application to human mitochondrial DNA. *Genetics*, **152**, 1079–1089.

Sluys R (1999) Global diversity of land planarians (Platyhelminthes, Tricladida, Terricola): a new indicator-taxon in biodiversity and conservation studies. *Biodiversity and Conservation*, **8**, 1–19.

Smith CI, Farrell BD (2005) Range expansion in the flightless longhorn cactus beetles, *Moneilema gigas* and *Moneilema armatum*, in response to Pleistocene climate changes. *Molecular Ecology*, **14**, 1025–1044.

Sunnucks P, Hales DF (1996) Numerous transposed sequences of mitochondrial cytochrome oxidase I–II in aphids of the Genus *Sitobion* (Hemiptera, Aphididae). *Molecular Biology and Evolution*, **13**, 510–524.

Sunnucks P, Tait N (2001) Velvet worms: tales of the unexpected. *Nature Australia*, **27**, 61–69.

Sunnucks P, Curach N, Young A *et al.* (2000a) Reproductive biology of the onychophoran *Euperipatoides rowelli*. *Journal of the Zoological Society of London*, **250**, 447–460.

Sunnucks P, Wilson ACC, Beheregaray LB, Zenger K, French J, Taylor AC (2000b) SSCP is not so difficult: the application and utility of single-stranded conformation polymorphism in evolutionary biology and molecular ecology. *Molecular Ecology*, **9**, 1699–1710.

Swofford DL (2002) PAUP*. *Phylogenetic Analysis Using Parsimony (* and Other Methods)*, Version 4. Sinauer Associates, Sunderland, Massachusetts.

Tajima F (1989) Statistical method for testing neutral mutation hypothesis by DNA polymorphism. *Genetics*, **123**, 585–589.

Templeton AR (1998) Nested clade analyses of phylogeographic data: testing hypotheses about gene flow and population history. *Molecular Ecology*, **7**, 381–397.

Templeton AR, Crandell KA, Sing CF (1992) A cladistic analysis of phenotypic associations with haplotypes inferred from restriction endonuclease mapping and DNA sequence data. III. *Genetics*, **132**, 619–633.

Thompson JD, Gibson TJ, Plewniak F, Jeanmougin F, Higgins DG (1997) The CLUSTAL_X windows interface: flexible strategies for multiple sequence alignment aided by quality analysis tools. *Nucleic Acids Research*, **25**, 4876–4882.

Trewick SA, Wallis GP (2001) Bridging the 'beech-gap': New Zealand invertebrate phylogeography implicates pleistocene glaciation and pliocene isolation. *Evolution*, **55**, 2170–2180.

Watterson GA (1975) On the number of segregating sites in genetical models without recombination. *Theoretical Population Biology*, **7**, 256–276.

Winsor L (1998a) Aspects of taxonomy and functional histology in terrestrial flatworms (Tricladida: Terricola). *Pedobiologia*, **42**, 412–432.

Winsor L (1998b) The Australian terrestrial flatworm fauna (Tricladida: Terricola). *Pedobiologia*, **42**, 457–463.

Woodman J, Ash JE, Rowell DM (2006) Population structure in a saproxylic funnelweb spider (Hexathelidae: *Hadronyche*) along a forested rainfall gradient. *Journal of Zoology*, **268**, 325–333.

Mark Blacket, postdoctoral researcher currently working on insect evolution, made contributions to all aspects of this study. Jody Taylor contributed to the work during her honours year, and Chester Sands and Ryan Garrick during their related PhD programmes. Sherryn Ciavaglia was awarded a Genetics Society of Australia scholarship to work on this project. Noel Tait researches organisms blessed with slime; along with David Rowell and Paul Sunnucks he has been engaged in comparative phylogeography of log-dwelling invertebrates. Alexandra Pavlova is a postdoctoral researcher who has published mainly on bird phylogeography: she introduced a number of important perspectives and analyses here. This is a publication of the Australian Centre for Biodiversity: Analysis, Policy & Management.

Appendix I

Geographic location of sampling logs and distribution of sampled haplotypes (see also Figs 1 and 2). Abbreviations for the catchment-based micro-regions are HCR, Harolds Cross Region; LG, Lake George; MO, Molonglo; ESR, Eastern Slopes Region; ESR-Ba, northern part of ESR located in Ballalaba subcatchment; ESR-Je, southern part of ESR located in Jerrabatgulla subcatchment; AR, Anembo Region; PSR, Pikes Saddle Region; DU, Deua; NU, Numeralla; BR, Badja Region; BO, Bredbo. Some collecting points (logs) were located along the fire trails dividing two subcatchments, in these cases logs were assigned to the border between two regions (X–Y where X was the subcatchment in which the log was slightly more located). Letters under 'Haplotype distribution' correspond to the haplotypes (Fig. 2), numbers after them indicate number of individuals sharing the same haplotype if multiple haplotypes sampled

Species	Region	LogID	Easting	Northing	No. of individuals	Haplotype distribution
A. lucasi	HCR-LG	F06	730866	6080898	10	O9, P1
		F07	729978	6080317	9	O
		F08	729930	6079239	12	O
	HCR	C22	733107	6075111	7	J3, K2, O2
		C23	731898	6074621	1	K
		C29	738293	6076446	3	J
		C32	738413	6072888	1	J
		C33	738497	6071151	1	O
		C38	731305	6074312	5	N1, O4
		N05	731462	6075081	2	M1, O1
	MO	C24	730660	6068381	4	K1, O3
		N40	727854	6067476	1	O
	MO-HCR	C39	730870	6074422	2	O
		C41	730870	6074422	5	O
	ESR-MO	D06	727289	6051973	1	A
		F11	727295	6050861	8	A
		F12	726950	6052850	4	A
		VM06	726277	6055202	1	F
	MO-ESR	C26	726997	6061253	6	E
		C27	727831	6064434	3	E
		VM01	726479	6053627	1	A
	ESR-Ba	C35	735859	6067743	1	O
		C37	727880	6060577	2	E
		D05	727909	6053519	1	A
		E01	728211	6053368	1	A
		E03	728479	6054379	1	A
		E07	728479	6054379	1	A
		E08	728479	6054379	2	A
		E09	728479	6054379	1	A
		E11	729138	6051235	2	A
		E12	729138	6051235	4	A
		E13	729138	6051235	2	A
		E14	728749	6049598	3	A
		E15	728749	6049598	1	A
		E32	728211	6053368	2	A
		E34	728211	6053368	1	A
		F09	729148	6048183	7	A
		F10	728395	6050423	15	A
		J24	732367	6065826	1	B
		SH03	728009	6053077	2	A
		SH04	728063	6053116	2	A
		SH05	729453	6047421	5	A
		SH06	729470	6047359	1	A
		SH10	728265	6053964	1	A
		W01	727809	6054072	1	F
		W02	727937	6054149	3	F
	ESR-Je	W05	729733	6041910	3	B
		T01	726600	6027900	1	B
		T02	725600	6028100	2	B

Appendix I *Continued*

Species	Region	LogID	Easting	Northing	No. of individuals	Haplotype distribution
A. lucasi (continued)	AR	A01	724200	6030500	2	B
		B57	723821	6038704	1	C
		C09	726380	6024559	1	T
	AR-ESR	B40	724513	6030393	1	B
		C19	726742	6033885	3	E
		C21	727520	6039756	2	B1, E1
	ESR-AR	C08	726169	6024696	5	T
		C18	725373	6031813	4	E
		J05	725685	6025408	4	T
	PSR	C10	734762	6018234	1	T
		C11	734869	6017391	3	D2, T1
		D11	738296	6015628	2	T
	PSR-DU	C15	741696	6017393	1	Q
	NU-PSR	T12	728950	6014010	1	T
	PSR-NU	D13	730047	6014307	2	T
		D33	729939	6014239	1	T
	NU	B53	727963	6009606	1	S
	BR-NU	D22	732297	6004208	1	R
	NU-BR	B79	731538	6008349	1	T
		D18	731421	6010725	1	T
	BR	B63	727751	5993605	1	G
		D34	725806	5991858	1	I
		B02	726700	5994000	1	H
C. coerulea	HCR-LG	C42	731714	6082735	1	n
		F02	732703	6083497	1	o
		F03	731002	6081334	2	o
		F04	731587	6082437	1	o
		F05	731140	6082063	1	o
		F06	730866	6080898	3	o
		F07	729978	6080317	17	o
		F08	729930	6079239	5	l1, o4
	HCR	C22	733107	6075111	1	o
		C38	731305	6074312	3	o
		J28	733336	6071781	1	m
		J29	733874	6070844	1	k
		N05	731462	6075081	22	o
	MO	C24	730660	6068381	3	l1, n1, o1
	MO-HCR	C39	730870	6074422	6	n1, o5
		C41	730870	6074422	2	n
	ESR-MO	J17	727232	6051641	1	h
		J18	726890	6060976	1	h
	MO-ESR	J10	726843	6058520	2	o
	ESR-Ba	C34	737503	6069542	1	n
		E11	729138	6051235	1	h
		E13	729138	6051235	1	h
		E30	728749	6049598	1	h
		E32	728211	6053368	1	h
		E34	728211	6053368	6	h
		F09	729148	6048183	5	h1, o4
		F10	728395	6050423	3	h1, o2
		H07	728612	6047616	4	h
		J22	737614	6068214	1	n
		SH05	729453	6047421	2	h
		W01	727809	6054072	3	e
		W02	727937	6054149	1	h

Appendix I *Continued*

Species	Region	LogID	Easting	Northing	No. of individuals	Haplotype distribution
C. coerulea (continued)	ESR-Je	T08	729200	6037300	1	q
		W05	729733	6041910	1	h
		W07	729696	6030477	2	g1, h1
		T01	726600	6027900	2	h
		T02	725600	6028100	1	h
	AR-ESR	C19	726742	6033885	4	p1, c1, g1, h1
		C21	727520	6039756	1	f
		T04	725500	6033800	2	h
		T05	725500	6033800	3	h
	ESR-AR	D04	727864	6033766	1	q
	ESR-AR	J01	724562	6029972	1	h
		J02	724561	6029971	1	h
		J05	725685	6025408	3	h
	PSR	B97	732638	6018172	1	c
		C10	734762	6018234	9	c8, d1
		C11	734869	6017391	4	c
		C12	736150	6015726	1	a
		D11	738296	6015628	4	a
		T14	730900	6023300	4	i
	NU-PSR	C01	727060	6015142	3	a
		T12	728950	6014010	7	a
	PSR-NU	D33	729939	6014239	5	a4, d1
		L30	730200	6014400	1	a
	NU	B26	730483	6003381	1	j
		B53	727963	6009606	1	a
		B87	725956	6011246	5	a
	BR-NU	D23	732310	6004758	4	j
		B23	725560	5993230	1	j
	NU-BR	B66	725755	5995935	1	j
		B79	731538	6008349	2	a1, d1
		D26	723269	5993466	1	j
	BR	B03	726700	5993900	4	j
		B15	728640	5996032	1	j
		B28	732771	6001915	1	j
		B60	728600	5993700	1	j
	NU-BO	B89	726156	6015478	1	b
		C02	727068	6015157	2	a

Appendix II

Descriptive statistics for COI sequences for *Artioposthia lucasi* and *Caenoplana coerulea*

Species	Codon position	No. of bases	No. of variable bases	Proportion			
				A	C	G	T
A. lucasi (n = 197)	1st	121	0	0.28	0.08	0.31	0.33
	2nd	121	3	0.17	0.19	0.24	0.41
	3rd	122	29	0.17	0.03	0.12	0.68
	all	364	32	0.21	0.10	0.22	0.47
C. coerula (n = 192)	1st	120	0	0.30	0.08	0.28	0.34
	2nd	120	0	0.16	0.18	0.24	0.42
	3rd	121	20	0.18	0.02	0.13	0.67
	all	361	20	0.21	0.09	0.22	0.47

Appendix III

Geographic definition of subcatchment-based geographic regions and the boundaries between them, and relative values of population subdivision for (a) *Artioposthia lucasi* and (b) *Caenoplana coerulea*. Lines indicate boundaries between regions; colours represent relative value of pairwise φ_{ST}: blue, φ_{ST} from 0 to 0.2 (recent or contemporary gene flow); yellow, φ_{ST} from 0.21 to 0.05 (restricted gene flow); and red, φ_{ST} from 0.51 to 1 (long-term historic isolation). Abbreviations are as follows: LG, Lake George; HCR, Harolds Cross Region; ESR, Eastern Slopes Region (Ba, Ballalaba; Je, Jerrabatgulla); PSR, Pikes Saddle Region; DU, Deua; BR, Badja Region; NU, Numeralla; BO, Bredbo; AR, Anembo Region; MO, Molonglo

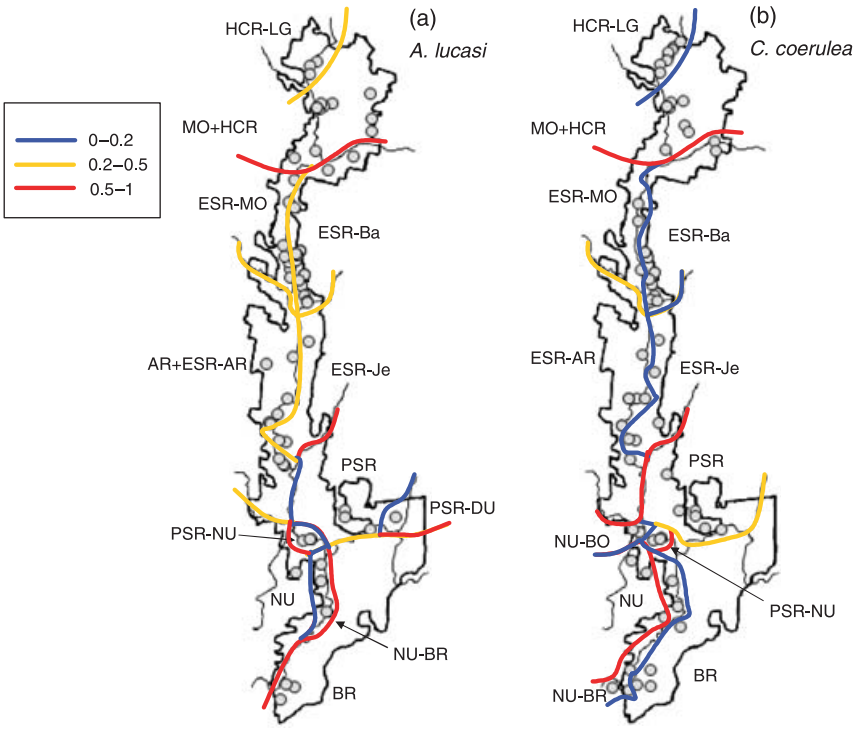

Appendix IV

Pairwise population φ_{ST} values for subcatchment-based microregions and their boundaries within *Artioposthia lucasi*. Numbers in parentheses indicate sample sizes; an asterisk indicates $P < 0.05$; negative estimates of φ_{ST} are replaced by zero. Grouping individuals into microregions explained 76% of all genetic diversity (total $\varphi_{ST} = 0.76$, $P < 0.001$)

Region	HCR-LG (31)	MO+HCR (32)	ESR-MO (24)	ESR-Ba (63)	ESR-Je (6)	ESR-AR (23)	PSR (6)	PSR-DU (1)	PSR-NU (4)	NU (1)	NU-BR (3)	BR (3)
HCR	—											
MO+HCR	0.28*	—										
ESR-MO	0.91*	0.77*	—									
ESR-Ba	0.93*	0.84*	0.2*	—								
ESR-Je	1*	0.8*	0.27	0.31*	—							
ESR-AR	0.78*	0.64*	0.31*	0.56*	0.37*	—						
PSR	0.92*	0.69*	0.57*	0.75*	0.65*	0.02	—					
PSR-DU	0.99	0.71	0.72	0.86	1	0.12	0.02	—				
PSR-NU	1*	0.77*	0.79*	0.88*	1*	0.29	0.11	1	—			
NU	1	0.78	0.78	0.89	1	0.23	0.12	1	1	—		
NU-BR	0.98*	0.73*	0.74*	0.86*	0.93*	0.2	0	0.2	0.11	0.38	—	
BR	0.98*	0.72*	0.6*	0.78*	0.89*	0.26	0.4*	0.72	0.86	0.77	0.68*	—

Appendix V

Pairwise population φ_{ST} values for subcatchments-based microregions and their boundaries within *Caenoplana coerulea*. Numbers in parentheses indicate sample sizes; an asterisk indicates $P < 0.05$; negative estimates of φ_{ST} are replaced by zero. Grouping individuals into microregions explained 75% of all genetic diversity (total $\varphi_{ST} = 0.75$, $P < 0.001$)

Region	HCR-LG (31)	MO+HCR (39)	ESR-MO (4)	ESR-Ba (30)	ESR-Je (7)	ESR-AR (16)	PSR (23)	PSR-NU (16)	NU (7)	NU-BR (9)	BR (7)	NU-BO (3)
HCR	—											
MO+HCR	0.01	—										
ESR-MO	0.72*	0.58*	—									
ESR-Ba	0.69*	0.66*	0	—								
ESR-Je	0.9*	0.86*	0.22	0.08*	—							
ESR-AR	0.82*	0.8*	0.22*	0.11*	0	—						
PSR	0.84*	0.84*	0.59*	0.61*	0.6*	0.54*	—					
PSR-NU	0.98*	0.95*	0.9*	0.81*	0.89*	0.81*	0.3*	—				
NU	0.93*	0.9*	0.62*	0.68*	0.67*	0.62*	0.13*	0.07	—			
NU-BR	0.87*	0.85*	0.5*	0.6*	0.55*	0.55*	0.6*	0.8*	0.54*	—		
BR	0.98*	0.94*	0.84*	0.75*	0.85*	0.76*	0.79*	0.98*	0.83*	0.07	—	
NU-BO	0.98*	0.94*	0.72*	0.73*	0.77*	0.69*	0.16	0.17	0	0.62*	0.98*	—